

## Water in the Half Shell: Structure of Water, Focusing on Angular Structure and Solvation

KIM A. SHARP AND JANE M. VANDERKOOI\*

*E. R. Johnson Research Foundation and Department of Biochemistry and Biophysics, School of Medicine, University of Pennsylvania, Philadelphia, Pennsylvania 19104*

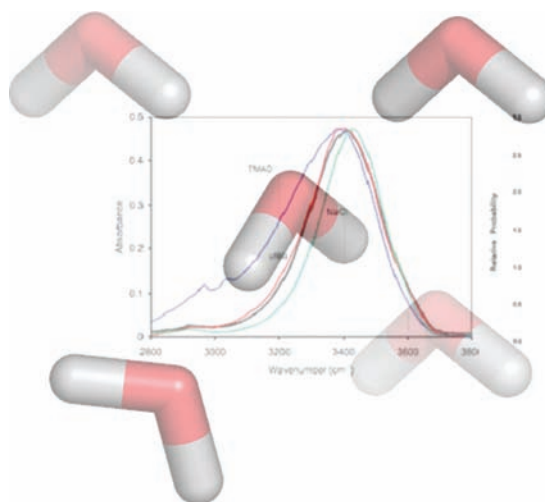
RECEIVED ON MAY 14, 2009

### CON SPECTUS

Water is a highly polar molecule, consisting of a very electronegative atom, oxygen, bonded to two weakly electropositive hydrogen atoms with two lone pairs of electrons. These features give water remarkable physical properties, some of which are anomalous, such as its lower density in the solid phase compared with the liquid phase. Its ability to serve as both a hydrogen bond donor and hydrogen bond acceptor governs its role as a solvent, a role that is of central interest for biological chemists.

In this Account, we focus on water's properties as a solvent. Water dissolves a vast range of solutes with solubilities that range over 10 orders of magnitude. Differences in solubility define the fundamental dichotomy between polar, or hydrophilic, solutes and apolar, or hydrophobic, solutes. This important distinction plays a large part in the structure, stability, and function of biological macromolecules. The strength of hydrogen bonding depends on the H–O···O H-bond angle, and the angular distribution is bimodal. Changes in the width and frequency of infrared spectral lines and in the heat capacity of the solution provide a measure of the changes in the strength and distribution of angles of the hydrogen bonds. Polar solutes and inorganic ions increase the population of bent hydrogen bonds at the expense of the more linear population, while apolar solutes or groups have the opposite effect.

We examine how protein denaturants might alter the solvation behavior of water. Urea has very little effect on water's hydrogen bond network, while guanidinium ions promote more linear hydrogen bonds. These results point to fundamental differences in the protein denaturation mechanisms of these molecules. We also suggest a mechanism of action for anti-freeze (or thermal hysteresis) proteins: ordering of water around the surface of these proteins prior to freezing appears to interfere with ice formation.



### Introduction

The study of water has had a long history, starting in the first millenium BCE with Thales of Miletus' statement that "the principle of all things is water". Water has remarkable physical properties, some of which are anomalous. Many of these anomalies occur at conditions far from standard temperature and pressure and thus are of interest mostly for physical chemists. For biologists, a

major concern is the properties of water as a solvent, because the structure and function of biological macromolecules depend upon liquid water. Both OH–O distances and angles contribute to H-bonding strength; however changes in H-bond angle distribution provide a quantitative explanation of the positive and negative hydration heat capacity ( $C_p$ ) of, respectively, apolar and polar solutes or protein groups. Experimentally, changes in

H-bonding are inferred from the OH stretch frequency of infrared, lowering as H-bonding strength increases. How water changes in various biological milieus, that is, in the presence of salt, cryoprotectants, denaturants, and protein surfaces, is the subject of this Account.

## The Water Molecule

Water consists of a highly electronegative oxygen atom bonded to two weakly electropositive hydrogen atoms. This results in a highly polar molecule that can donate H-bonds through the positively charged H atoms, accept H-bonds through the negatively charged O atom, and more generally make strong electrostatic interactions. From a structural perspective, a key advance was the determination of the structure of Ice I<sub>h</sub>, Figure 1a.<sup>1</sup> Ice I<sub>h</sub> is the form found at moderate temperature and pressure, and it is the familiar form of ice. Bragg's work revealed the now famous tetrahedral ice lattice structure. Each water molecule has four hydrogen-bonded first neighbors at a distance of 2.75 Å, two as H-bond donor and two as H-bond acceptor. The four neighbors are placed at the vertices of a tetrahedron, with mutual separations of 4.5 Å. Ice I<sub>h</sub> is a very open structure with a high degree of radial and angular ordering that has played a large part in our thinking about liquid water, since the latter's structure is still not fully characterized. Since there are two hydrogen atoms per molecule, it seems intuitive that in liquid water a molecule would ideally donate two H-bonds, as in ice I<sub>h</sub>. It is less obvious that the optimal number of H-bonds to accept is two. Indeed the number and geometry of H-bonds made by water in the liquid state remains the focus of many studies.

## Liquid Water

**Radial Structure.** An advance in understanding liquid water structure was the determination, through X-ray and neutron scattering experiments, of O–O, H–H, and O–H radial distribution functions ( $g(r)$ ).<sup>2–4</sup> Remarkably, these show that much of the tetrahedral ice lattice persists in liquid water: from the oxygen–oxygen radial distribution (local density) function,  $g_{OO}(r)$ , the nearest neighbors, with a density peak at 2.8–2.9 Å, are just slightly more distant than in those ice I<sub>h</sub> (Figure 2). There is also a residual, though very broad, peak of density at 4.5 Å diagnostic of tetrahedral ordering between waters in the first coordination shell. The radial distribution functions do however indicate extensive differences between ice and liquid water. The number of nearest neighbors (coordination number), defined as the integral of  $g_{OO}(r)$  through the first peak to the first minimum is about 4.5–4.7, significantly higher than that in ice,<sup>5</sup> although still low compared with other

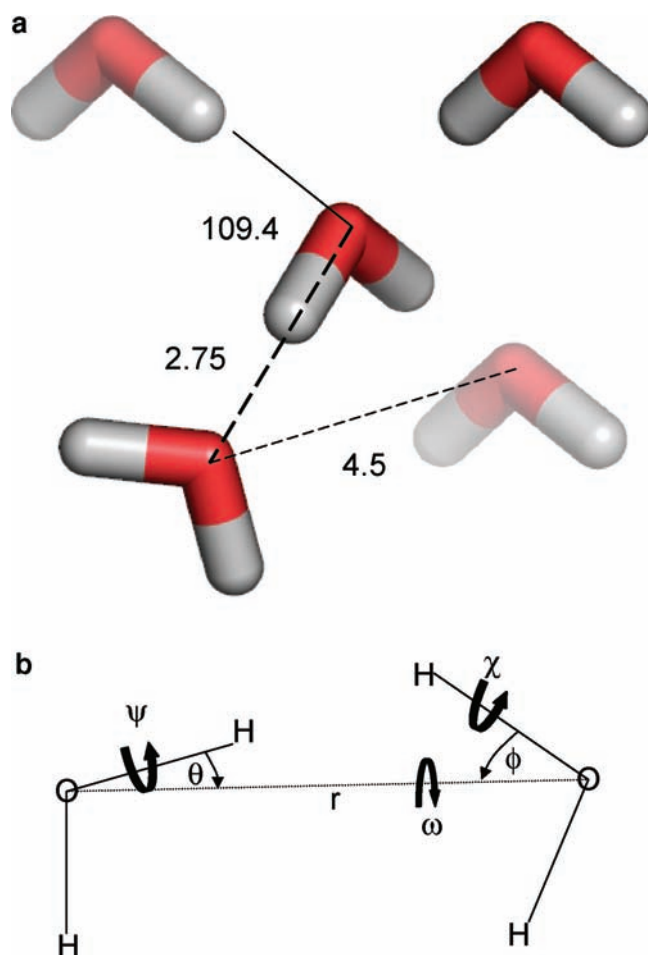


**FIGURE 1.** (a) Tetrahedral arrangement and dimensions in the ice I<sub>h</sub> lattice and (b) some geometric definitions for the water pair:  $r$  is the distance between the two O atoms,  $\theta$  is the H–O–O angle for the one H atom of the four that makes the smallest angle,  $\phi$  is the corresponding angle for the H-atom of the other water that makes the minimum H–O–O angle,  $\psi$  and  $\chi$  are the two angles the second H atoms make with the H–O–O plane, and  $\omega$  is the dihedral angle along the O–O line.

liquids. Typical small molecule organic liquids have coordination numbers of 6–10. Thus water, like ice, is an open structured liquid with a high degree of angular ordering. However, in the liquid there is a considerable amount of density lying between the ice first and second shell positions (at 2.75 and 4.5 Å, respectively). This density is too high at the first minimum position (at  $\sim 3.4$  Å) to be simply the overlap of broadened ice-derived first and second shell densities.

Radial distribution functions can be obtained directly from low-angle X-ray/neutron scattering experiments and have provided a wealth of information over a wide range of temperatures and pressures. They have been less informative about structure changes accompanying solvation: precise experimental studies using neutron scattering combined with hydrogen/deuterium isotope substitution find little change in  $g(r)$ 's

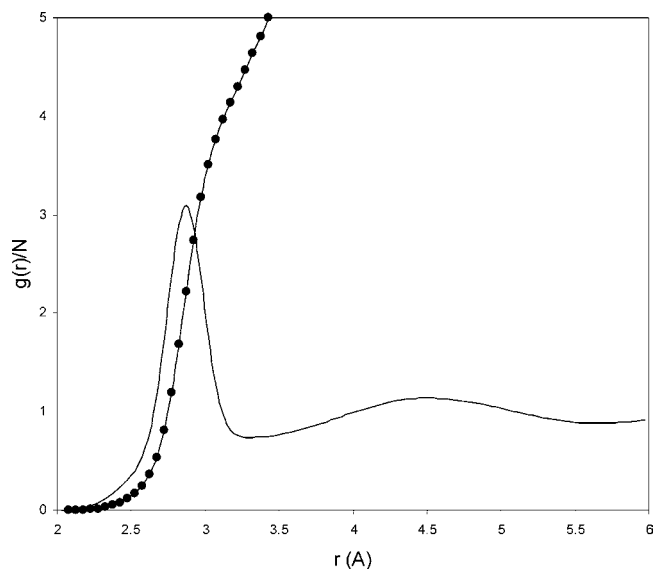


**FIGURE 2.** Radial distribution function  $g_{oo}(r)$  and integrated number of waters (●) for liquid water at 298 K and 1 atm. Data from Soper and Phillips.<sup>59</sup>

upon addition of a solute.<sup>6,7</sup> In particular, the distance between nearest neighbor waters around ionic and apolar solutes appears to be quite conserved at 2.75–2.9 Å.

**Angular Structure.** Angular structure of liquid water is only indirectly available from scattering and spectroscopy techniques, often with significant help from computer simulations. There are several ways to characterize angular structure. Measures of tetrahedrality derived from water center triplet positions<sup>8</sup> have been used to good effect in characterizing the anomalous structural properties of pure water over a range of temperature and pressure values<sup>9</sup> but are rather insensitive to solute effects. Although water around apolar groups becomes more ordered, as shown by the negative entropy of solvation, little difference in tetrahedrality is seen.<sup>8</sup> A tetrahedrality measure based on distances rather than angles<sup>10</sup> has, however, been shown to pick up differences in water structure induced by thermal hysteresis proteins.<sup>11</sup> The spatial density function measures the relative density of waters around a central water oriented in a fixed reference frame; that is, it is the local density distribution as a function of distance and polar coordinate,  $g(r, \phi, \theta)$ .<sup>12,13</sup> Through elegant experimental work combined with extensive modeling,  $g(r, \phi, \theta)$  has been extracted from neutron scattering data.<sup>14,15</sup> Simulation and experiment give excellent agreement. A couple of important structural features of liquid water are revealed by this measure (Figure 3). First, the orientation of the two H-bond acceptor waters in the first coordination shell is much more defined than that of the two (or more?) H-bond donor molecules. Second, there is significant density of water placed

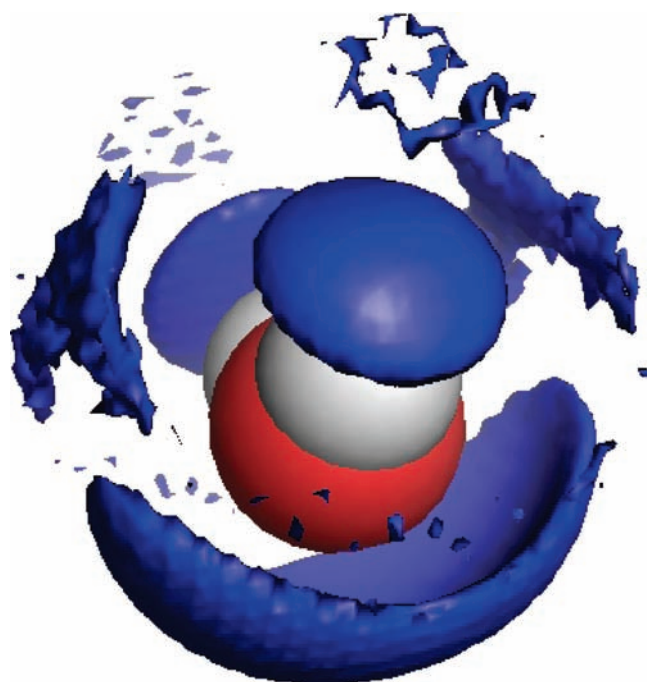


**FIGURE 3.** Spatial position function  $g(r, \phi, \theta)$  of liquid water at 298 K, 1 atm, simulated with the TIP3P water model.

interstitially to the first coordination shell slightly further out at  $\sim 3.2$ – $3.8$  Å, but significantly closer than the second shell at 4.5 Å. It is this water density, halfway between the original first and second shell positions in ice  $I_h$ , (the half shell of our title) resulting from the partial collapse of the open ice structure, which accounts for the significant density at the first minimum of  $g_{oo}(r)$  and the increase in coordination number of 0.5–0.8 waters upon melting. These interstitial water peaks are greatly enhanced at higher pressures by further collapse.<sup>13,14</sup>

The third major way of quantifying angular structure is through the H–O···O angle,  $\theta$ , formed between two waters, choosing the H atom of the four that gives the smallest angle (Figure 1b).<sup>16</sup> For convenience, we refer to this as the H-bond angle, although there is no formal requirement for the two waters to be actually H-bonded. Liquid water can be viewed, with respect to ice  $I_h$ , as a randomly perturbed network of H-bonds with the principle perturbation occurring in this H-bond angle coordinate.<sup>16–20</sup> The value of  $\theta$  proves to be very sensitive to changes in water structure, and changes in  $\theta$  have been linked quantitatively to thermodynamic, physical, and solvation properties of water. In Figure 4, we show simulation results for water using the TIP4P model.<sup>21</sup> The joint O–O distance ( $r$ ), H–O–O angle probability distribution between water pairs,  $p(r, \theta)$ , is plotted. Taking ice  $I_h$  as a reference, we see that the first coordination shell of four waters is largely intact, broadening in the  $r$  direction and moving to a

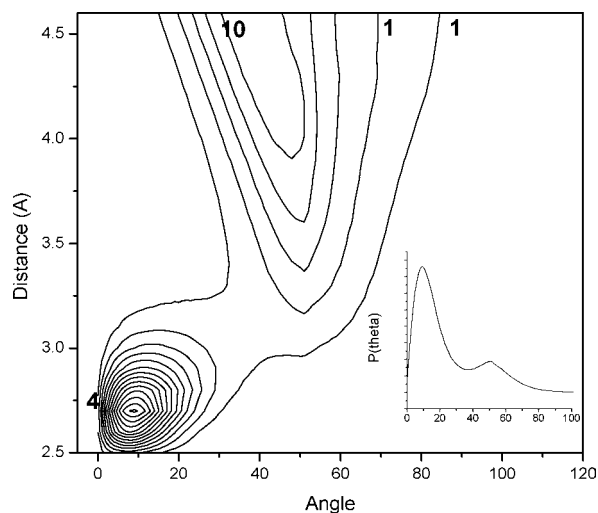


**FIGURE 4.** Distance and H-bond angle probability distribution,  $p(r, \theta)$ , for water pairs in liquid water at 298 K, 1 atm, simulated with the TIP4P water model. Numbers on the figure indicate the position and number of waters in the  $p(r, \theta)$  for ice  $I_h$ . Inset shows the angle probability function  $p(\theta)$  for all water pairs with  $r \leq 3.5$  Å.

somewhat less linear mean H-bond angle of  $12^\circ$  due to thermal motion. The integrated population of this more linear H-bond angle peak remains close to 4. Meanwhile the second coordination shell is extensively restructured. Significant density moves in, some (ca. 0.5–0.8 waters) within the first coordination shell. This forms a population of more bent H-bonds (mean angle  $\sim 57^\circ$ ) resulting in a bimodal H-bond angle distribution, with a saddle point around  $3.2$  Å and  $38^\circ$ . The figure inset ( $p(\theta)$  for all waters up to the first minimum in  $g_{OO}(r)$  at  $r = 3.5$  Å) emphasizes that the bimodal distribution exists within the first shell. The higher angle peak is formed by the persistent fifth water in the first shell forced to make a bent H-bond with the central water, one of the other four first shell waters, or both. This bimodal distribution has been confirmed with simulations using other water models including SPCE and F3C,<sup>11,22,23</sup> and it is consistent with spectroscopic studies discussed below. A satisfying geometric explanation for  $\theta \approx 57^\circ$  of the high angle peak is that the fifth water is forced by the four quasi-tetrahedral first coordination shell waters to approach the central water on a tetrahedron face, as shown by the spatial position function<sup>13,15</sup> (see Figure 3) and so makes a H-bond at close to half the tetrahedral angle. Robinson et al. attribute many of the anomalous physical properties of water to the presence of this half shell water and its structural and thermodynamic lability.<sup>24</sup>

**Perturbations in Angular Structure by Solutes.** The bimodal distribution of H-bond angles in liquid water is sensitive to a variety of perturbations, significantly more so than the radial structure.<sup>25</sup> Angular distortion is a softer mode of

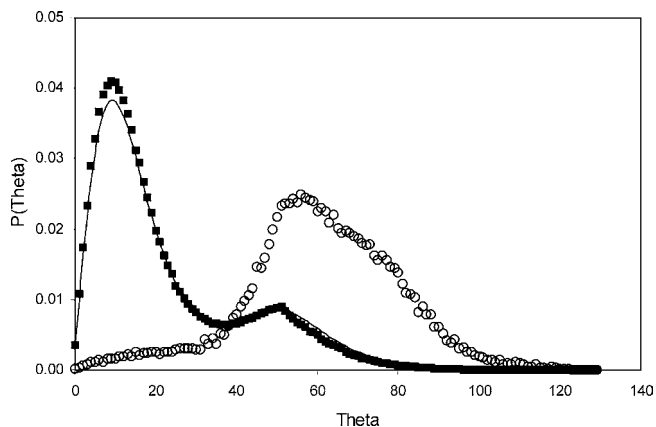


**FIGURE 5.** H-bond angle probability function for all water pairs with  $r \leq 3.5$  Å for pure water (—), first shell of NaCl (○), and first shell of TMAO (■) at 298 K, 1 atm simulated with the TIP4P water model.

deformation than distance distortion. Because of this, different angular structures can lie within quite similar radial distribution envelopes. The relative insensitivity of scattering data to solutes can be attributed partly to this. The bimodal distribution of water–water H-bond angles is also sensitive to solute type. In a series of studies on small molecules, proteins, and nucleic acids, it was found that polar solutes and inorganic ions increase the population of bent H-bonds at the expense of the more linear population, while apolar solutes or groups do the reverse.<sup>22,26–31</sup> Figure 5 shows an example of solute effects on the first shell water–water H-bond angle distribution for trimethylamineoxide (TMAO, apolar) and NaCl (polar). The physical explanation for these solute effects is straightforward. Water is a highly cohesive, strongly interacting network of H-bonding groups. A weakly interacting apolar solute can only insert itself by displacing the more weakly coordinated half shell water that makes the larger H-bond angle. Conversely, polar groups with their strong electrostatic fields tend to radially align solvating waters, so they must make more strained H-bonds with each other.

For the two dozen or more solutes and half dozen proteins looked at so far, the water–water H-bond angle population remains bimodal, with peak and saddle positions unchanged.<sup>23,31</sup> Only relative populations of the two peaks change. While current empirical water potentials are imperfect, these shifts in bimodal H-bond angle distribution have been seen with three water models, TIP3P, TIP4P, and F3C;<sup>11,22,26,31</sup> the phenomenon is robust.

Changes in water–water H-bond angle can be related to other water properties. They provide a quantitative explanation of the positive and negative hydration heat capacity ( $C_p$ ) of, respectively, apolar and polar solutes or protein groups.<sup>31</sup> Apolar groups increase the population of more linear



water–water H-bonds with larger water–water interaction energy. The fluctuation in this energy is also larger, resulting in a net increase in the  $C_p$  of the solvating water. The converse is true for polar solutes: waters making more bent water–water H-bonds interact more weakly and so produce smaller fluctuations of energy, lowering  $C_p$ . Effects of solutes are largely confined to the first shell, which explains empirical observations that hydration  $C_p$  effects are proportional to polar and apolar solvent-accessible areas of solutes.<sup>32,33</sup>

An example of subtle solvation effects revealed by these water–water H-bond angle changes is provided by so-called hydrophobic ions. Inorganic ions are of course highly polar. Larger ions of the alkyl-ammonium type, for example, tetramethyl-ammonium ( $\text{TMA}^+$ ), are classed as hydrophobic ions, because, although soluble in water, they increase water's  $C_p$  rather than decrease it. This reversal of behavior is seen in the effect on the angular structure. While  $\text{K}^+$  promotes more bent H-bonds,  $\text{TMA}^+$  actually promotes more linear H-bonds.<sup>34</sup>

The distance/H-bond angle distribution function,  $p(r, \theta)$ , is actually a two-dimensional subset of the six-dimensional (one distance, five angles) function that completely specifies the mutual arrangement of two water molecules of fixed geometry (Figure 1b). We focus on the H-bond angle  $\theta$  since changes in the other four angles are small and reveal little about solvation.<sup>34</sup> The reason  $\theta$  is the most informative of the angle coordinates is that combined with  $r$ , it specifies the two (of the nine total) atom–atom distances between two waters that have greatest contribution to pair interaction energy, namely, the O–O interaction and the closest O–H interaction.

A general conclusion from these studies is that the more bent H-bonds are weaker, more labile to perturbation by temperature and solutes. This view is reinforced by the results emerging from infrared spectroscopy of hydrated solutes and proteins, discussed below.

**Broken H-bonds? Two States in Liquid Water?** Two perennial yet controversial ideas are found intertwined in literature on liquid water. The first is water as a mixture of two (or more) distinguishable states, dating back to flickering cluster and iceberg models.<sup>35,36</sup> The bimodal distribution of water interaction energies seen right from the first computer simulations of liquid water by Rahman and Stillinger<sup>5</sup> were taken by some as confirmation of this. Literature on the two state idea is too extensive to discuss here, except to note that strong favoring evidence appears to be isosbestic points in the Raman spectroscopy.<sup>37</sup> This interpretation has recently been challenged.<sup>38</sup> The second idea is that liquid water contains a mixture of made and broken H-bonds. Related to the second idea is the debate about how many H-bonds a water mole-

cule makes in the liquid state. Again, this literature is so voluminous we can only touch on the major point. Based on liquid water's larger coordination number, and the partial collapse of the open ice structure, many people argue that a water molecule must be making *at least* four H-bonds as in ice  $\text{I}_h$ , maybe more. This is our view. Recent X-ray absorption spectroscopy (XAS) experiments have been interpreted by Wernet et al., with significant help from simulation, to mean the opposite: water makes less H-bonds in the liquid than in ice, as few as two.<sup>39</sup> This radical result has been challenged by Smith et al., based on additional XAS experiments.<sup>40</sup>

Given the results of H-bond angle analysis discussed in the preceding section, the bimodal distribution of H-bond angles and that temperature and solutes perturb relative amounts but not positions of these two water angle populations, it is tempting to talk about two states of water or to map the low-angle and high-angle populations onto the made and broken H-bonds of earlier discussions. However, several things should be pointed out. First, the angle analysis does not show two states of water in the pure liquid. There is on average one kind of water, but it simultaneously makes low- and high-angle H-bonds. There is perhaps a mixture of two *interactions* but not of water states. Second, the analysis is based on continuous distributions, there are no *a priori* definitions of what a made H-bond is. The bimodal behavior emerges from this analysis, but it is best to view liquid water as a continuously deformed network of H-bonds, as in the random network models of water that underpin our analysis.<sup>21</sup> In our opinion, there has been a largely fruitless debate on criteria for broken H-bonds in the literature. See for example the insightful discussion in Kumar et al.,<sup>23</sup> who also use and discuss the continuous water–water distance/H-bond angle distribution function,  $p(r, \theta)$ . The application of a “cutoff” for H-bonds risks throwing out the baby with the bath water, and we believe definition issues lie behind the controversy over the interpretations of XAS experiments.

**Angular and Distance Dependence of Water's IR Stretching Absorption.** Water's ability to H-bond has a large influence on its vibrational spectroscopic profile. As noted above, the oxygen of a water molecule is electronegative, and it withdraws electrons from H, leaving H unshielded. The oxygen of a neighboring water molecule, by having lone-pair electrons, has electrons to donate such that its electrons can interact with H. The distributions of electrons affect the force constant between O and H. With increased H-bonding strength, water's stretching frequencies go lower, while the bending frequency goes higher.<sup>41,42</sup> It follows that by exam-

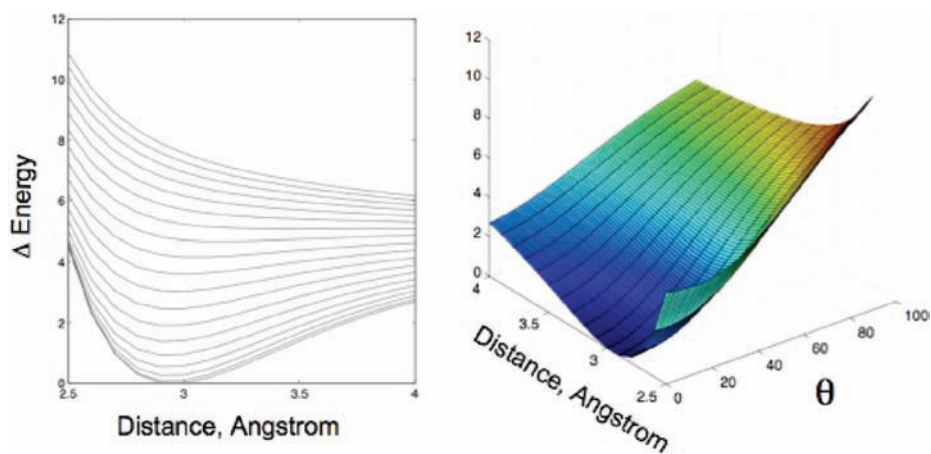


**FIGURE 6.** Water dimer energy (left) as a function of distance shown for 5° intervals of H-bond (HOO) angle (0° is the lowest energy curve) and potential energy surfaces (PES, right) for water dimer with fixed internal molecular geometry, showing energy dependence on O–O distance and H-bond angle. All energies are in kcal/mol relative to minimum. Data obtained with acceptor water molecule and donor oxygen fixed in the plane of H-bond angle. The B3LYP DFT and 6-311++G(d,p) basis set with BSSE correction using Gaussian 03.

ining the IR of water, information on the H-bonding network can be obtained.

To demonstrate the orientation and distance dependence of H-bonding on IR absorption, we show quantum computations of the O–O bond of a water dimer (Figure 6, N. Scott, unpublished). Looking at an O–O distance of 2.8 Å, the approximate distance between O's in liquid water, a near linear H bond produces the lowest frequency. As the angle between OH and the plane defined by O and the acceptor water molecule increases, the minimum in the energy disappears. At high angle and long distances, H-bonding covalent interactions no longer are in play, and electrostatic interactions predominate. This is one set of data; other angles and distances have also been examined with the same general conclusion. Of course, water dimer calculations do not mimic the case for liquid water since, in liquid each water molecule interacts with more than one water molecule, as described above. But the results do show that the energy of H-bonding is a sensitive function of angle of the H-bond.

#### IR/MD Studies of Water with Ions and Small Solutes.

Using this as a background, when correlated with angular dependence computations, IR measurements provide a semi-quantitative picture of water arrangement around the solute. In the IR works that are cited here, the sample is 95% D<sub>2</sub>O and 5% H<sub>2</sub>O. At this ratio, the HOH concentration is about 0.14 M whereas the HOD concentration is ~5.3 M. Therefore, the OH stretch band that is observed arises from HOD that is decoupled from water's other stretching vibration. In Figure 7, the OH stretch absorption region is shown for neat water and water containing TMAO or NaCl.<sup>43</sup> The sample containing TMAO shows absorption shifting to lower frequency, indicating stronger H-bonds and consistent with the simula-

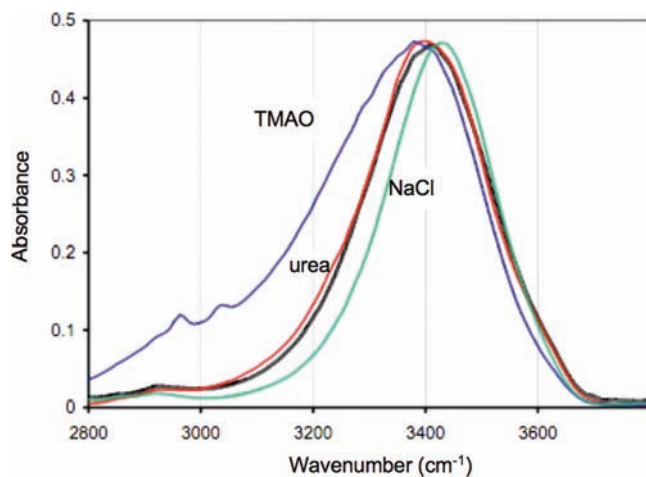


**FIGURE 7.** OH stretch absorption of 95% D<sub>2</sub>O, 5% H<sub>2</sub>O upon addition of solutes: black, neat water; blue, 5 M TMAO; green, 5 M NaCl; red, 5 M urea.

tions of TMAO solutions (Figure 5), which showed increased linear H-bonding.<sup>25</sup> The OH stretch band of water containing NaCl shifts to higher frequency (Figure 7), showing that the salt promotes nonlinear H-bonding. Again the simulations confirm this (Figure 5).

Recently, this experimental work has been extended to the Hofmeister series of ions.<sup>44</sup> These ions are ranked based upon an over 100 year observation that they have differing ability to cause protein aggregation. Using an effective two-state hydrogen-bonding model to interpret the temperature excursion infrared response of the O–H stretch of aqueous salt solutions, the sequence of anions that promote linear H-bonding followed the Hofmeister ranking as follows: PO<sub>4</sub><sup>3-</sup> > SO<sub>4</sub><sup>2-</sup> > HPO<sub>4</sub><sup>2-</sup> > Cl<sup>-</sup> > Br<sup>-</sup> > NO<sub>3</sub><sup>-</sup>. For cations, the order was Mg<sup>2+</sup> > Li<sup>+</sup> > Na<sup>+</sup> ≥ K<sup>+</sup>; again the band shift of OH stretch indicates linear H-bonding for the kosmotrope Mg<sup>2+</sup> and bent for the

chaotrope  $K^+$ .<sup>44</sup> Ions that bind weakly to water are large, and the charge is distributed over several atoms, as for  $NO_3^-$ . When the charge is larger and on one locus, the ions ability to order water is the greatest.<sup>45</sup>

In biology, compounds that contain hydroxyl groups are used to preserve biological samples under extreme cold or heat. Glycerol, used to stabilize proteins for storage at low temperature, can serve as an example. As glycerol concentration increases, water's H-bonding network decreases, and finally water will no longer crystallize. This is evident in the IR spectrum of the OH stretch of glycerol/water mixtures, which shows no evidence of crystals even at 20 K.<sup>46</sup>

**IR/MD Studies of Water Solutions Containing Protein Denaturants.** Urea and guanidine salts have been used for 70 years to denature proteins in solution.<sup>47</sup> Despite many years of investigation, the exact mechanism by which guanidinium, that is,  $Gdm^+$  ( $C(NH_2)_3^+$ ), or urea ( $CO(NH_2)_2$ ) destabilize folded structures of proteins is still a matter of debate. A mechanism proposed for protein denaturation is that these substances directly interact with the protein amide group or some part of the side chain. This direct interaction model has long-standing evidence.<sup>47</sup> However, the evidence does not necessarily rule out the possibility that these substances also affect water since by altering the H-bonding network of water, the native, folded state of a given protein could become no longer energetically favorable and the equilibrium could shift toward unfolding.

The vibrational OH absorption band of water reveals whether  $GdmHCl$  and urea changes water H-bonding. Urea has no large effect on the IR absorption spectrum of water.<sup>43</sup> The lack of effect on water indicates that H-bonding between water and urea is very much the same as water H-bonding to each other. This conclusion has also been reached by time-resolved IR<sup>48</sup> and neutron diffraction.<sup>49</sup> In Figure 8, absorption spectra of neat liquid water, ice, and  $Gdm^+Cl$  solutions are shown. In contrast to urea,  $Gdm^+$  promotes low-frequency absorption of the OH band, indicating that it produces stronger, more linear "ice-like" H-bonding. While this does not preclude that  $Gdm^+$  binds to components of the protein, stronger H-bonding of water would promote higher partitioning of hydrophobic groups in the aqueous phase, and therefore the altered water structure would contribute to the destabilization of proteins.<sup>50</sup> The structures of  $Gdm^+$  and urea are different. In addition to difference in charge,  $Gdm^+$  is planar and symmetrical. Urea is more floppy and is expected to replace water molecules without a major disruption of the water H-bonding network.

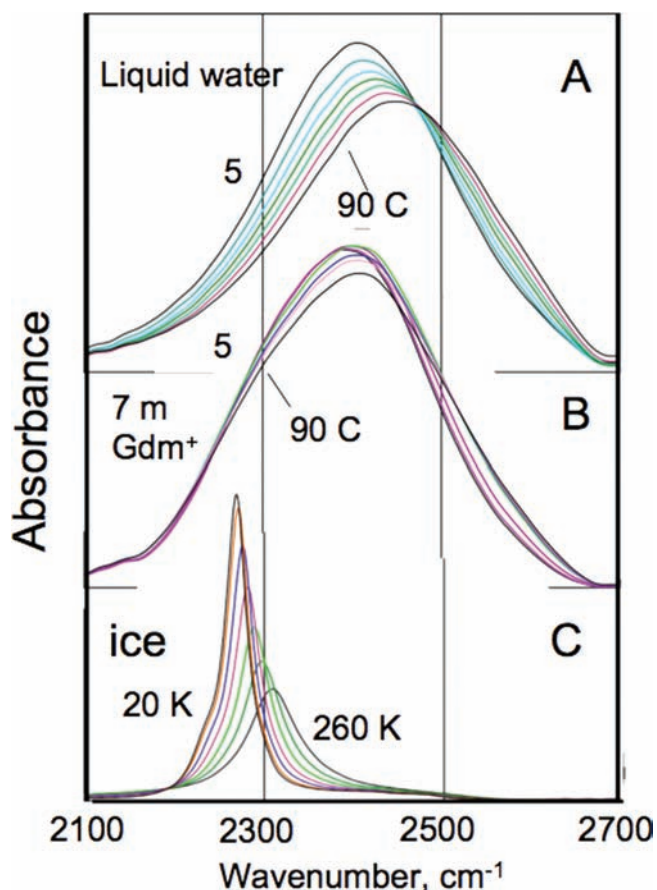


**FIGURE 8.** OH stretch of 95%  $D_2O$ , 5%  $H_2O$  from 5 to 90 °C: (A) water with no salt; (B) 7 m guanidinium chloride from similar data;<sup>50</sup> (C) ice from 260 to 20 K from similar data.<sup>60</sup>

**Amide Absorption as Influenced by H-Bonding to Water.** The amide group of proteins gives rise to two strong absorption bands that are widely used experimentally to study protein conformation. The amide I band, absorbing near 1650  $cm^{-1}$ , arises mainly from  $C=O$  stretching vibration with smaller contributions from the out-of-phase  $C-N$  stretching vibration, the  $C-C-N$  deformation, and the  $N-H$  in-plane bend. In proteins, the frequency and extinction coefficient depends on the secondary structure of the backbone since these are functions of the H-bonding and dipolar coupling between amide groups.<sup>51</sup> The amide II mode is the out-of-phase combination of the  $NH$  in-plane bend and the  $C-N$  stretching vibration.

Both amide I and II mode frequencies are sensitive to H-bonding. Strengthening the H-bond between a donor and the  $C=O$  group shifts the amide I band lower. H bonding from the  $N-H$  and an acceptor in the solvent shifts the amide II band higher. The amide I stretch frequency for amide groups H-bonded to water is temperature dependent, since as temperature decreases water's H-bonding strength increases.<sup>42,52,53</sup> The temperature dependence of the frequency of water



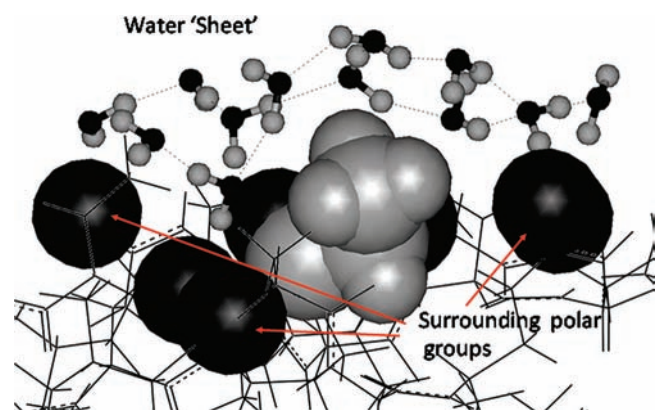


**FIGURE 9.** Structure of water around flounder antifreeze protein. Residue Ala16 defines the center of the ice nuclei binding site. Simulated water structure using TIP3P water model.<sup>55</sup>

H-bonded amides indicates the residues of proteins that are exposed to water. The band is dynamically broadened by the fluctuating field of H-bonded water as measured by time-resolved vibration spectroscopy.<sup>54</sup>

**IR/MD Studies of Proteins That Bind Ice.** Water–water H-bond angle changes have been used to study hydration of thermal hysteresis or antifreeze proteins (AFPs).<sup>11,55,56</sup> These proteins act as biological cryo-protectants by depressing the freezing point by binding ice nuclei and inhibiting their growth. A major conundrum is how such proteins can recognize and bind ice nuclei in a large 55 M excess of chemically identical liquid water. Here the sensitivity of the water–water H-bond angle measure has revealed subtle but systematic differences between ice-binding and non-ice-binding surfaces of proteins. Ice-binding surfaces have more linear (i.e., more ice-like) water–water H-bonding in their solvating waters. Interestingly, this effect is mediated by both polar and apolar groups on the protein, arranged in such a fashion that even polar groups have more linear water–water H-bonds, a reversal of the pattern seen in small solutes and other protein groups. It thus seems that AFPs are either recognizing ice by differences in angular structure or perturbing water’s angular structure so as to promote ice binding (see Figure 9). Antifreeze activity is not specific for stereochemistry of the protein, consistent with the nonstereospecific ice surface.<sup>57</sup> The amide I region of AFP from winter flounder does not shift in vibrational frequency during water’s phase transition of liquid to solid.<sup>58</sup> This suggests that AFP perturbs water structure prior to ice formation.

## In Summary

Water is a highly polar molecule consisting of a very electronegative atom, oxygen, bonded to weakly electroposi-

tive hydrogen atoms and having two lone-pair electrons. Its ability to be both a H-bond donor and a H-bond acceptor governs its role as a solvent. Insights on water’s interactions with solutes and at surfaces of biomacromolecules can be further obtained by considering the angular dependence of H-bonding.

Supported by NIH Grant GM 48130. We thank Nathan Scott for helpful discussion and data of Figure 6.

## BIOGRAPHICAL INFORMATION

**Kim A. Sharp** was born in Prague, The Czech Republic. He was awarded his Ph.D. from the University of British Columbia, Vancouver, in 1985. He uses theory and computer simulations to study the structure of water, electrostatic and hydrophobic interactions, and the solvation of proteins and nucleic acids. Current work is focused on the mechanism of antifreeze proteins.

**Jane M. Vanderkooi** grew up in Amherst, South Dakota, and Herman, Minnesota. She received a Ph.D. from St. Louis University, Missouri, in 1971. She studies protein dynamics using spectroscopy and is currently studying water’s influence on protein stability.

## FOOTNOTES

\* To whom correspondence should be addressed. E-mail: vanderko@mail.med.upenn.edu.

## REFERENCES

- Bragg, W. H. The crystal structure of ice. *Proc. Phys. Soc. London* **1921**, *34*, 98–103.
- Narten, A.; Levy, H. Liquid water: Molecular correlation functions from x-ray diffraction. *J. Chem. Phys.* **1971**, *55*, 2263–2269.
- Bosio, L.; Chen, S.; Teixeira, J. Isochoric temperature differential of the x-ray structure factor and structural rearrangements in low-temperature heavy water. *Phys. Rev. A* **1983**, *27*, 1468–1475.
- Soper, A. K. The radial distribution functions of water and ice. *Chem. Phys.* **2002**, *258*, 121–137.
- Rahman, A.; Stillinger, F. Molecular dynamics study of liquid water. *J. Chem. Phys.* **1971**, *55*, 3336–3359.
- Turner, J.; Soper, A. The effect of apolar solutes on water structure: Alcohols and tetraalkylammonium ions. *J. Chem. Phys.* **1994**, *101*, 6116–6125.
- Turner, J.; Soper, A.; Finney, J. Ionic versus apolar behavior of the tetramethylammonium ion in water. *J. Chem. Phys.* **1995**, *102*, 5438–5443.
- Chau, P.; Hardwick, A. A new order parameter for tetrahedral configurations. *Mol. Phys.* **1998**, *93*, 511–518.
- Errington, J.; Debenedetti, P. Relationship between structural order and the anomalies of liquid water. *Nature* **2001**, *409*, 318–321.
- Medvedev, N.; Naberukhin, Y. Shape of the Delaunay simplexes in dense random packings of hard and soft spheres. *J. Non-Cryst. Solids* **1987**, *94*, 402–406.
- Smolin, N.; Daggett, V. Formation of ice-like water structure on the surface of an antifreeze protein. *J. Phys. Chem. B* **2008**, *112*, 6193–6202.
- Svishchev, I.; Kusalik, P. Structure in liquid water: A study of spatial distribution functions. *J. Chem. Phys.* **1993**, *99*, 3049–3061.
- Svishchev, I. M.; Zassetsky, A.; Kusalik, P. Solvation structures in three dimensions. *Chem. Phys.* **2000**, *258*, 181–186.
- Soper, A.; Ricci, M. Structures of high-density and low-density water. *Phys. Rev. Lett.* **2000**, *84*, 2881–2884.
- Soper, A. K. Probing the structure of water around biological molecules: Concepts, constructs and consequences. *Physica B* **2000**, *276*, 12–16.
- Henn, A. R.; Kauzmann, W. Equation of state of a random network, continuum model of liquid water. *J. Phys. Chem.* **1989**, *93*, 3770–3783.



- 17 Pople, J. *Proc. R. Soc. London* **1961**, A205, 163.
- 18 Sceats, M. G.; Stavola, M.; Rice, S. A. A zeroth order random network model of liquid water. *J. Chem. Phys.* **1979**, *70*, 3927–3938.
- 19 Sceats, M. G.; Rice, S. A. A random network model calculation of the free energy of liquid water. *J. Chem. Phys.* **1980**, *72*, 6183–6191.
- 20 Rice, S. A.; Sceats, M. G. A random network model for water. *J. Phys. Chem.* **1981**, *85*, 1108–1119.
- 21 Gallagher, K.; Sharp, K. A. A new angle on heat capacity changes in hydrophobic solvation. *J. Am. Chem. Soc.* **2003**, *125*, 9863–9870.
- 22 Raschke, T.; Levitt, M. Nonpolar solutes enhance water structure within hydration shells while reducing interactions between them. *Proc. Natl. Acad. Sci. U.S.A.* **2005**, *102*, 6777–6782.
- 23 Kumar, R.; Schmidt, J.; Skinner, J. Hydrogen bonding definitions and dynamics in liquid water. *J. Chem. Phys.* **2007**, *126*, 204107.
- 24 Cho, H.; Singh, S.; Robinson, G. Understanding all of water's anomalies with a nonlocal potential. *J. Chem. Phys.* **1997**, *107*, 7979–7988.
- 25 Madan, B.; Sharp, K. Changes in water structure induced by a hydrophobic solute proved by simulation of the water hydrogen bond angle and radial distribution functions. *Biophys. Chem.* **1999**, *78*, 33–41.
- 26 Madan, B.; Sharp, K. Heat capacity changes accompanying hydrophobic and ionic solvation: A Monte Carlo and random network model study. *J. Phys. Chem.* **1996**, *100*, 7713–7721.
- 27 Madan, B.; Sharp, K. Molecular origin of hydration heat capacity changes of hydrophobic solutes: Perturbation of water structure around alkanes. *J. Phys. Chem. B* **1997**, *101*, 11237–11242.
- 28 Sharp, K. A.; Madan, B. Hydrophobic effect, water structure, and heat capacity changes. *J. Phys. Chem. B* **1997**, *101*, 4343–4348.
- 29 Vanzi, F.; Madan, B.; Sharp, K. Effect of the protein denaturants urea and guanidinium on water structure: A structural and thermodynamic study. *J. Am. Chem. Soc.* **1998**, *120*, 10748–10753.
- 30 Madan, B.; Sharp, K. A. Hydration heat capacity of nucleic acid constituents determined from the random network model. *Biophys. J.* **2001**, *81*, 1881–1887.
- 31 Gallagher, K. R.; Sharp, K. A. Analysis of thermal hysteresis protein hydration using the random network model. *Biophys. Chem.* **2003**, *105*, 195–209.
- 32 Spolar, R. S.; Livingstone, J. R.; Record, M. T., Jr. Use of liquid hydrocarbon and amide transfer data to estimate contributions to protein folding. *Biochemistry* **1992**, *31*, 3947–3955.
- 33 Gomez, J.; Hilser, V.; Xie, D.; Freire, E. The heat capacity of proteins. *Proteins* **1995**, *22*, 404–412.
- 34 Gallagher, K. R.; Sharp, K. A. A new angle on heat capacity changes in hydrophobic solvation. *J. Am. Chem. Soc.* **2003**, *125*, 9853–9860.
- 35 Frank, H. S.; Wen, W. Y. Structural aspects of ion-solvent interaction in aqueous solutions: A suggested picture of water structure. *Discuss. Faraday Soc.* **1957**, *24*, 133.
- 36 Nemethy, G.; Scheraga, H. Structure of water and hydrophobic bonding. I. A model for the thermodynamic properties of liquid water. *J. Chem. Phys.* **1962**, *36*, 3382–3400.
- 37 Walrafen, G. E. Raman spectral studies of the effects of temperature on water structure. *J. Chem. Phys.* **1967**, *47*, 114–126.
- 38 Smith, J. D.; Cappa, C. D.; Wilson, K. R.; Cohen, R. C.; Geissler, P. L.; Saykally, R. J. Unified description of temperature-dependent hydrogen-bond rearrangements in liquid water. *Proc. Natl. Acad. Sci. U.S.A.* **2005**, *102*, 14171–14174.
- 39 Wernet, P.; Nordlund, D.; Bergmann, U.; Cavalleri, M.; Odelius, M.; Ogasawara, H.; Naslund, L.; Hirsch, T. K.; Ojamae, L.; Glatzel, P.; Pettersson, L. G.; Nilsson, A. The structure of the first coordination shell in liquid water. *Science* **2004**, *304*, 995–999.
- 40 Smith, J.; Cappa, C.; Wilson, K.; Messer, B.; Cohen, R.; Saykally, R. Energetics of hydrogen bond network rearrangements in liquid water. *Science* **2004**, *306*, 851–853.
- 41 Jeffrey, G. A. *An Introduction to Hydrogen Bonding*; Oxford University Press: New York, 1997.
- 42 Vanderkooi, J. M.; Dashnau, J. L.; Zelent, B. Temperature excursion infrared (TEIR) spectroscopy used to study hydrogen bonding between water and biomolecules. *Biochim. Biophys. Acta* **2005**, *1749*, 214–233.
- 43 Sharp, K. A.; Madan, B.; Manas, E. S.; Vanderkooi, J. M. Water structure changes induced by hydrophobic and polar solutes revealed by simulations and infrared spectroscopy. *J. Chem. Phys.* **2001**, *114*, 1791–1796.
- 44 Nucci, N. V.; Vanderkooi, J. M. Effects of salts of the Hofmeister series on the hydrogen bond network of water. *J. Mol. Liq.* **2008**, *143*, 160–170.
- 45 Collins, K. D. Charge density-dependent strength of hydration and biological structure. *Biophys. J.* **1997**, *72*, 65–76.
- 46 Dashnau, J. L.; Nucci, N. V.; Sharp, K.; Vanderkooi, J. M. Hydrogen bonding and the cryoprotective properties of glycerol/water mixtures. *J. Phys. Chem. B* **2006**, *110*, 13670–13677.
- 47 Pace, C. N. Determination and analysis of urea and guanidine hydrochloride denaturation curves. *Methods Enzymol.* **1986**, *131*, 266–280.
- 48 Rezus, Y. L. A.; Bakker, H. J. Effect of urea on the structural dynamics of water. *Proc. Natl. Acad. Sci. U.S.A.* **2006**, *103*, 18417–18420.
- 49 Soper, A. K.; Castner, E. W.; Luzar, A. Impact of urea on water structure: A clue to its properties as a denaturant? *Biophys. Chem.* **2003**, *105*, 649–666.
- 50 Scott, J. N.; Nucci, N. V.; Vanderkooi, J. M. Changes in water structure induced by the guanidinium cation and implications for protein denaturation. *J. Phys. Chem. A* **2008**, *112*, 10939–10948.
- 51 Krimm, S.; Bandekar, J. Vibrational spectroscopy and conformation of peptides, polypeptides, and proteins. *Adv. Protein Chem.* **1986**, *38*, 181–364.
- 52 Manas, E. S.; Getahun, Z.; Wright, W. W.; DeGrado, W. F.; Vanderkooi, J. M. Infrared spectra of amide groups in  $\alpha$ -helical proteins: Evidence for hydrogen bonding between helices and water. *J. Am. Chem. Soc.* **2000**, *122*, 9883–9890.
- 53 Walsh, S. T. R.; Cheng, R. P.; Daggett, V.; Vanderkooi, J. M.; DeGrado, W. F. The hydration of amides in helices: A comprehensive picture from molecular dynamics, IR and NMR. *Protein Sci.* **2003**, *12*, 520–531.
- 54 Mukherjee, P.; Kass, I.; Arkin, I. T.; Zanni, M. T. Structural disorder of the CD3 $\zeta$  transmembrane domain studied with 2D IR spectroscopy and molecular dynamics simulations. *J. Phys. Chem. B* **2006**, *110*, 24740–24749.
- 55 Yang, C.; Sharp, K. Hydrophobic tendency of polar group hydration as a major force in type I antifreeze protein recognition. *Proteins* **2005**, *59*, 266–274.
- 56 Yang, C.; Sharp, K. A. The mechanism of the type III antifreeze protein action: A computational study. *Biophys. Chem.* **2004**, *109*, 137–148.
- 57 Pentelute, B. L.; Gates, Z.; Dashnau, J. L.; Vanderkooi, J. M.; Kent, S. B. H. Mirror image forms of snow flea antifreeze protein (sfAFP) prepared by total chemical synthesis have identical antifreeze activities. *J. Am. Chem. Soc.* **2008**, *130*, 9702–9707.
- 58 Zelent, B.; Bryan, M. A.; Sharp, K. A.; Vanderkooi, J. M. Influence of surface groups of proteins on water studied by freezing/thawing hysteresis and infrared spectroscopy. *Biophys. Chem.* **2009**, *141*, 222–230.
- 59 Soper, A. K.; Phillips, M. G. A new determination of the structure of water at 25-degrees-C. *Chem. Phys.* **1986**, *107*, 47–60.
- 60 Zelent, B.; Nucci, N. V.; Vanderkooi, J. M. Liquid and ice water and glycerol/water glasses compared by infrared spectroscopy from 295 to 12 K. *J. Phys. Chem. A* **2004**, *108*, 11141–11150.